PUBLICATIONS OF THE ASTRONOMICAL SOCIETY OF THE PACIFIC, **116**:762–777, 2004 August


# Observing Conditions at Mount Graham: Vatican Advanced Technology Telescope *UBVR* Sky Surface Brightness and Seeing Measurements from 1999 through 2003

VIOLET A. TAYLOR, ROLF A. JANSEN, AND ROGIER A. WINDHORST

Department of Physics and Astronomy, Arizona State University, Box 871504, Tempe, AZ 85287-1504; violet.taylor@asu.edu, rolf.jansen@asu.edu, rogier.windhorst@asu.edu

*Received 2004 April 27; accepted 2004 June 1; published 2004 July 28*

**ABSTRACT.** We present measurements of sky surface brightness and seeing on Mount Graham, obtained at the Vatican Advanced Technology Telescope (VATT) during 16 observing runs between 1999 April and 2003 December. We show that the sky surface brightness is significantly darker during photometric conditions and can be highly variable over the course of a single observing run, as well as from one run to the next, regardless of photometricity. In our photometric observations, we find an average low air mass ($\sec z < 1.2$) sky surface brightness of 22.00, 22.53, 21.49, and 20.88 mag arcsec$^{-2}$ in *U*, *B*, *V*, and *R*, respectively. The darkest run (2000 February in *U* and 2001 February in *BVR*) had an average sky surface brightness of 22.38, 22.86, 21.72, and 21.19 mag arcsec$^{-2}$ in *U*, *B*, *V*, and *R*, respectively. With these results, we show that under the best conditions, Mount Graham can compete with the darkest sites in Hawaii and Chile, thanks in part to the strict dark-sky ordinances in place in Tucson and Safford. We expect the sky over Mount Graham to be even darker than our 1999–2003 results during solar minimum (2006–2007). We find a significant improvement of about 0\".45 in our measured stellar FWHM after improvements to the telescope were made in summer and fall 2001. Stellar FWHM values are highly variable, with median *R*-band focus FWHM values in each observing run ranging from 0\".97 to 2\".15. Significant subarcsecond seeing was occasionally achieved, with values as low as 0\".65 FWHM in *R*. There may still be a significant telescope contribution to the seeing at the VATT, but nearby trees as high as the dome are currently the dominant factor.

## 1. INTRODUCTION

The Mount Graham International Observatory (MGIO) is located near Safford, Arizona, at an altitude of 10,400 feet (3170 m). It contains the Vatican Advanced Technology Telescope (VATT), the Heinrich Hertz Submillimeter Telescope, and the Large Binocular Telescope[1] (LBT; currently under construction, with first light expected in late 2004). The observing conditions at the MGIO site are important limiting factors on the efficiency of observing faint objects, and it is thus important to characterize them with observations at the existing telescopes, as well as the LBT. Therefore, in this paper we focus on two of the most important properties of an observing site—the sky surface brightness and the seeing—over the course of 4 yr.

Dark sites are in decreasing supply because of metropolitan development, but reasonably dark sites do still exist. Other observers have studied sky surface brightness values at other observing sites, particularly in the context of determining the effects of nearby city lights. Massey & Foltz (2000) measured the sky brightness in various directions of the sky at Kitt Peak and Mount Hopkins in 1988 and again in 1998 to determine the effects of increasing light pollution from the expansion of Tucson. They found that since 1988, the zenith *BV* sky brightness increased slightly by 0.1–0.2 mag arcsec$^{-2}$ at Kitt Peak. At a larger zenith distance of 60°, however, there was a 0.35 mag arcsec$^{-2}$ increase when pointing away from Tucson, and a 0.5 mag arcsec$^{-2}$ increase when pointing toward Tucson. They mention that this increase in sky brightness would be worse if Tucson did not have good outdoor lighting ordinances, which also exist in Safford. Although Mount Graham is near Safford, Safford is a much smaller city than Tucson, and MGIO is located at a much higher elevation than Kitt Peak and Mount Hopkins, with Tucson and Phoenix situated well below the horizon as viewed from the Mount Graham summit. Hence, city lights should not have as large an impact on the sky brightness at MGIO.

Other factors besides city lights impact sky brightness, such as the presence of atmospheric dust, forest fire smoke, cirrus, the solar cycle, air mass, the Galactic and ecliptic latitude of the observation, the phase and angular distance of the Moon from the observed object, and the altitude and geomagnetic latitude of the observing site. Benn & Ellison (1998) measured the sky brightness at La Palma from 1987 to 1996, finding that the sky was 0.4 mag arcsec$^{-2}$ brighter during solar maximum than solar minimum, and 0.25 mag arcsec$^{-2}$ brighter at an air

[1] See http://medusa.as.arizona.edu/lbto.

mass (sec $z$) of 1.5 than an air mass of 1.0 (at the zenith). Krisciunas (1997) measured the sky brightness at Mauna Kea in Hawaii and found that except for the solar cycle, the most important effect is random short-term variations over tens of minutes, which makes sky brightness measurements highly variable and difficult to compare between sites. To quantify the quality of sky brightness at Mount Graham, we present our sky surface brightness measurements from 1999 April to 2002 April at the VATT, compare our measurements to those known at Mount Hopkins, Kitt Peak, Mauna Kea, La Palma, ESO, and Cerro Tololo, and discuss how the variability of sky brightness due to the factors listed above impact our conclusions. We also compare our measurements to a theoretical sky brightness for Mount Graham (Garstang 1989) and investigate the effects of city lights and the variation of sky brightness with time of night.

The seeing of an astronomical site can be estimated by measuring the median full width at half-maximum (FWHM) of stars in images taken at that site. We have done this for Mount Graham by measuring the FWHM of stars in stacked galaxy images and in short-focus exposures taken at the VATT. This is only an estimate, because there are other factors in addition to atmospheric seeing that play a role in the stellar FWHM, such as telescope focus and telescope image quality due to mirror quality, telescope collimation, etc. The FWHM results presented in this paper are to be applied at face value to the VATT alone and do not necessarily reflect on the Mount Graham site or on the LBT site, since the VATT's specific location on the mountaintop makes it more susceptible to ground-layer seeing, particularly in northeasterly winds.

## 2. OBSERVATIONS

We have obtained *UBVR* surface photometry for 142 galaxies with the VATT 2K × 2K direct CCD imager. Typical exposure times were 2 × (600–1200) s in $U$, 2 × (300–600) s in $B$, 2 × (240–480) s in $V$, and 2 × (180–360) s in $R$. The CCD gain is 1.9 $e$ ADU$^{-1}$, and the read noise is 5.7 $e$. We binned the images 2 × 2, resulting in a pixel scale of 0″.375 pixel$^{-1}$. Individual images were stacked with integer shifts, as the point-spread function (PSF) is well sampled. Sky brightness values and FWHM values measured from stacked images are the signal-to-noise weighted average values from the individual images that make up the stack, which suffices to examine overall trends in the data. The details of our galaxy sample and galaxy surface photometry, in addition to the methods we used for data reduction and calibration, are presented in a separate data paper on our nearby-galaxy survey (V. Taylor et al. 2004, in preparation).

Observations were spread over nine runs between 1999 April and 2002 April, for a total of 49 usable nights. Defining photometric nights as those with zero-point magnitudes that vary no more than 3% throughout, 45% of the nights were photometric, 51% were mostly nonphotometric (with parts of the night possibly photometric until clouds moved in), and 4% were lost entirely to telescope problems. During nights on which clouds appeared toward the end of the night, we salvaged as much as possible from the part of the night that was photometric.

For comparison, additional focus exposure stellar FWHM values are presented for eight VATT observing runs between 2001 November and 2003 December, which were carried out independently by R. A. Jansen for other projects.

## 3. TRENDS IN SKY SURFACE BRIGHTNESS AT THE VATT

### 3.1. Measurements of the Sky

Sky values for each stacked galaxy image were calculated by finding the median of the median pixel value in each of 13 boxes, each 120 pixels wide, along the edges of the image. This was done to avoid including light from the galaxy, which was usually centered in the CCD. Taking the median values helps to reject stars and cosmic rays, which comprise a small percentage of the total number of pixels in the sky boxes. The average sky count rates for all stacked galaxy images were $0.41 \pm 0.01$ ADU s$^{-1}$ in $U$, $1.34 \pm 0.11$ ADU s$^{-1}$ in $B$, $2.64 \pm 0.10$ ADU s$^{-1}$ in $V$, and $4.26 \pm 0.15$ ADU s$^{-1}$ in $R$. Sky surface brightness values were photometrically calibrated using Landolt standards (Landolt 1992). We defined photometric nights as those with zero points that vary no more than 3% throughout the night, which defines the largest uncertainty in the calibrations.

### 3.2. Sky Surface Brightness Results

In Figure 1, the resulting *UBVR* sky surface brightness values for each stacked galaxy image are plotted versus the average air mass (sec $z$) of the individual images that comprise each stack. Each observing run is broken up into a separate panel for comparison. Stacked images that are composed solely of individual images taken during photometric conditions (change in magnitude zero point throughout the night $\lesssim$3%) are plotted as asterisks, while those composed of images taken during nonphotometric conditions are plotted as open circles. There is a clear, well-defined difference in sky surface brightness between these two conditions: nonphotometric nights have notably brighter skies, as expected, due to the presence of cirrus. There is a trend of increasing sky surface brightness with increasing air mass, which is also to be expected, although there does not appear to be a single consistent slope to this trend throughout all observing runs, even for photometric runs. It is also apparent from the plots in Figure 1 that the sky surface brightness is highly variable as a function of time, both over the course of a single run and from one run to the next. Since sky brightness is highly dependent on many factors, such as solar activity, atmospheric conditions, time since sunset, variable night-sky lines, and the location of the telescope pointing

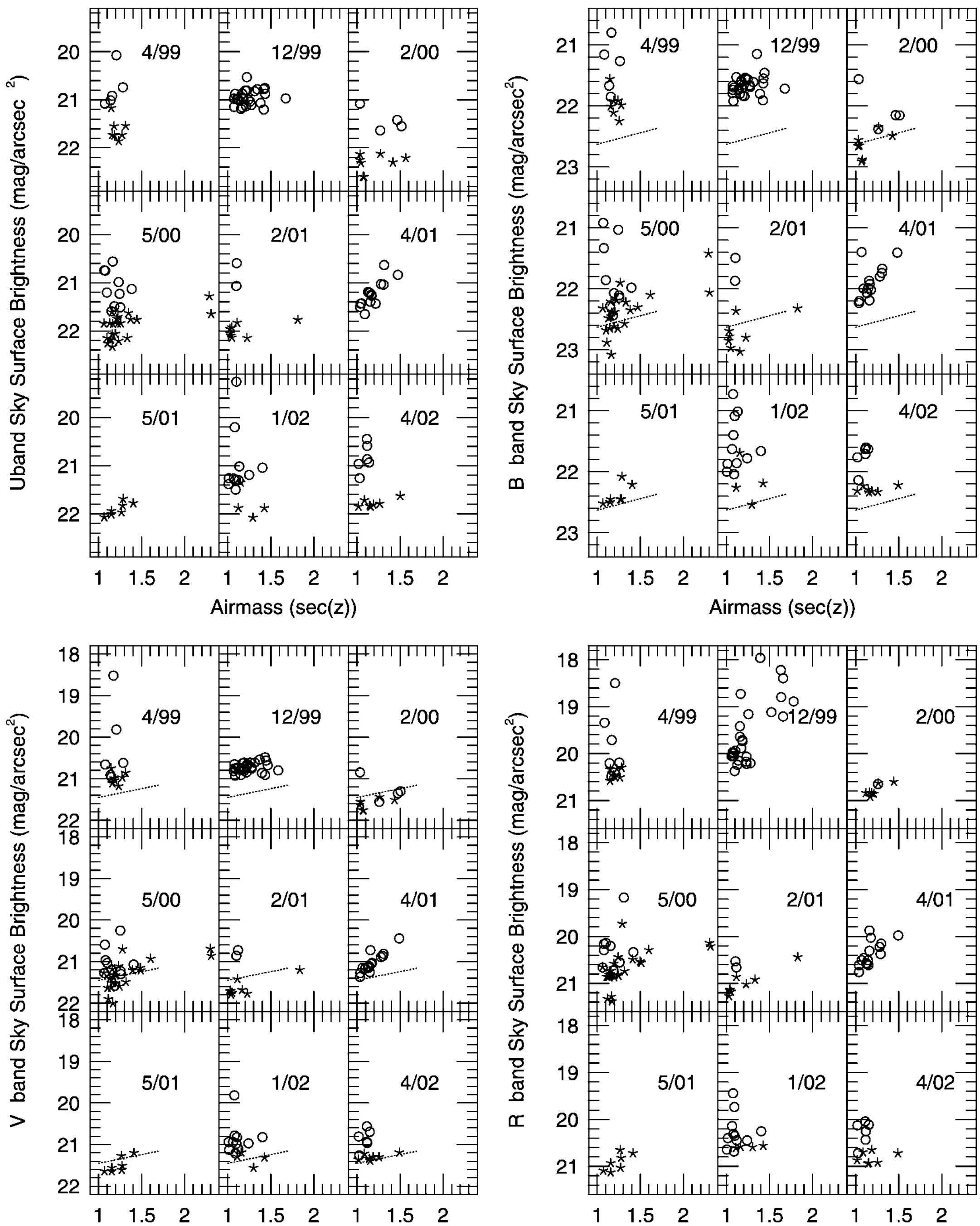


FIG. 1.—Sky surface brightness in stacked galaxy images taken at the VATT between 1999 April and 2002 April in *U*, *B*, *V*, and *R*. Each of our observing runs is indicated in a separate subpanel. Measurements obtained under nonphotometric conditions are represented by open circles, while measurements from photometric nights (zero-point variations $\lesssim 3\%$ throughout the night) are indicated by asterisks. Within a given run, the sky is brighter during nonphotometric than photometric conditions. The sky surface brightness can be highly variable on monthly, nightly, and tens-of-minutes timescales. Dotted lines represent the average values at Mount Hopkins/Kitt Peak (converted to broadband from spectrophotometry) over four nights in 1998 and 1999 (Massey & Foltz 2000), just before solar maximum (2000–2001).

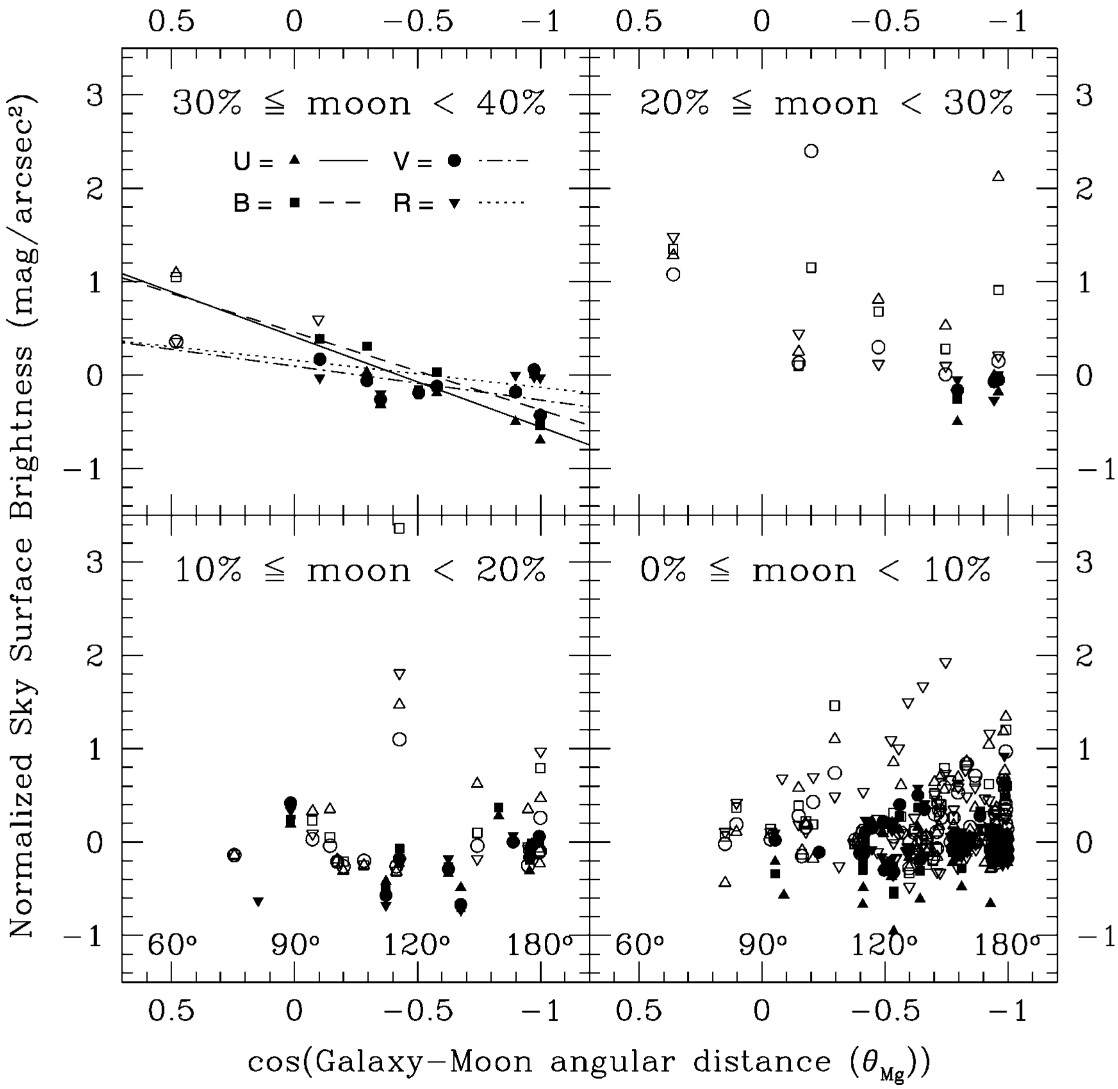


FIG. 2.—Dependence of the sky surface brightness, normalized to the median sky surface brightness for that observing run, on angular distance from the Moon for different Moon illuminations. Open symbols represent data that were taken during nonphotometric nights; filled symbols indicate data taken during photometric nights. Points are coded according to filter of observation, as indicated in the top left panel. A clear dependence on angular distance to the Moon is only seen for illumination $\gtrsim$20%. Straight lines represent linear least-squares fits to the data in each passband for data with $\sec z < 2$. The dependence on Moon distance is stronger at shorter wavelengths. In general, our galaxy images were taken well away from the Moon and mostly during dark nights ($\lesssim$4 days from new Moon), and thus the average sky surface brightness values presented in this paper are not strongly affected by the Moon.

with respect to nearby city lights, the Moon, zodiacal light, and the Galaxy itself, this variability is not surprising.

The effect of the Moon on the sky surface brightness of a given galaxy field is a complicated function of the phase of the Moon, the air mass ($\sec z$) of both the Moon and the galaxy position, the angular distance between the Moon and the galaxy ($\theta_{Mg}$), and the atmospheric extinction (Krisciunas & Schaefer 1991). We approximate the effect of the Moon on our sky surface brightness ($\mu$) results through a plot of the sky brightness of all stacked galaxy images versus $\cos\theta_{Mg}$, which is shown in Figure 2. We use $\cos\theta_{Mg}$ because the effects from the Moon on the sky brightness of a target away from the Moon may behave as a spherical harmonic, so some linear behavior in $\cos\theta_{Mg}$ may be expected. The secondary effects due to the air mass of the Moon and galaxy position and atmospheric extinction are not excluded here and are expected to be small compared to other large-scale variations in the overall sky surface brightness, as discussed above. The sky brightness values were normalized to the median sky brightness for the relevant observing run in order to remove large-scale seasonal effects. Four subpanels show different Moon phases ranging from a Moon illumination of 0% to 40%, which is the maximum illumination in our data. This plot shows that photometric nights (*indicated by filled symbols*) tend to have darker skies

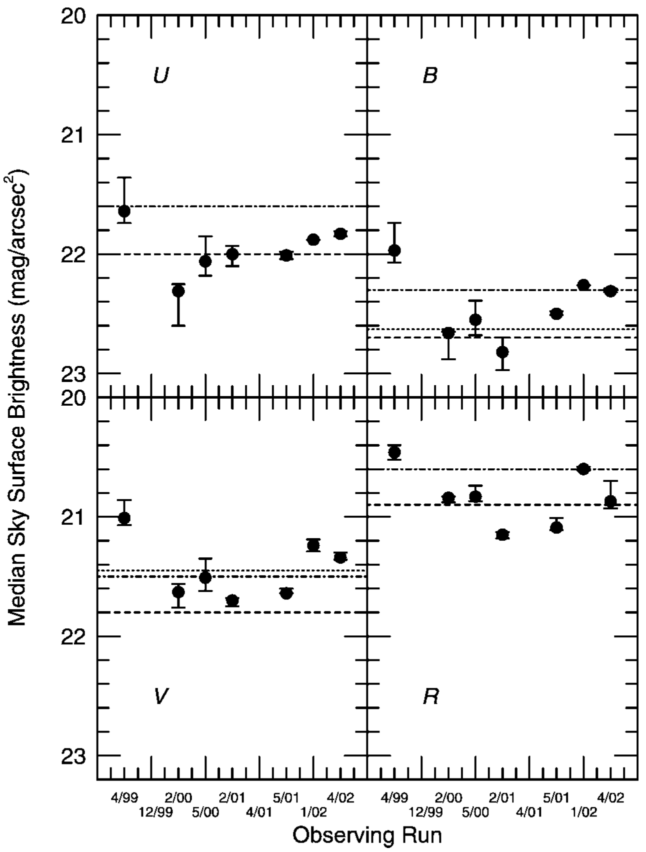


FIG. 3.—Median sky surface brightness of all photometric stacked galaxy images taken at the VATT with air mass (sec $z$) < 1.2, rejecting no more than one obvious outlier per data point. Error bars represent the 25%–75% quartile range. The horizontal lines represent the average sky surface brightness near zenith at Mount Hopkins and Kitt Peak, Arizona (*dotted line*; Massey & Foltz 2000; converted from spectrophotometry), Cerro Tololo, Chile (*dashed line*; Walker 1987; Walker & Schwarz 1987–1988 [see footnote 2]), and at La Palma, Canary Islands, Spain (*dot-dashed line*; Benn & Ellison 1998). A comparison with other sites is given in Table 1.

than nonphotometric nights (*open symbols*) and show a smaller scatter in sky surface brightness from one image to the next. Both photometric and nonphotometric exposures show no major trend with Moon angular distance within the scatter for Moon illumination ≤20%. There may be a slight antitrend of increasing sky surface brightness at 180° from the Moon, visible in the panel for Moon illumination ≤10%, which could be the result of sunlight back-scattering off of the atmosphere. A stronger trend of increasing sky surface brightness with decreasing Moon angular distance is apparent when Moon illumination is ≥20%. We applied a linear least-squares fit of

$$\mu = m \cos \theta_{\mathrm{M}g} + b \tag{1}$$

to this trend for the mostly photometric data in the panel with Moon illumination ≥30% (eliminating points with air mass >2) and determined slopes of 0.97 in *U*, 0.83 in *B*, 0.36 in *V*, and 0.29 in *R*. Thus, as expected, there is a stronger dependence on Moon angular distance for shorter wavelengths. There are only a small number of galaxy images (~5) that are affected by the Moon within the scatter of these plots, leading us to the conclusion that our median sky surface brightness values are largely unaffected by moonlight.

Solar maximum occurred around 2000–2001, in the middle of the time spanned by our observations, which could have raised the sky surface brightness by several tenths of a magnitude with respect to the sky surface brightness at solar minimum. For instance, Benn & Ellison (1998) saw an increase in sky brightness of 0.4 mag in *UBVR* from solar minimum to solar maximum at La Palma. We therefore expect the sky surface brightness to be fainter than these results by a similar amount during the upcoming solar minimum (2006–2007).

The dotted lines in Figure 1 (*B* and *V* panels) represent an estimate of the dependence of the sky surface brightness on air mass at Kitt Peak and Mount Hopkins, as measured by Massey & Foltz (2000), for comparison. Zenith values (air mass = 1.00) were derived by taking the average of the Massey & Foltz measurements at both locations, which consisted of one exposure in each passband at Mount Hopkins in 1998 November and four exposures in each passband at Kitt Peak over three nights in 1999 November (all of which were just before solar maximum, like our earlier runs—however, our later runs are closer to the solar maximum peak, and thus will be brighter). We calculated an average high air mass sky surface brightness by taking the average of four exposures in each passband at Mount Hopkins at zenith distances of 34°–53° and six exposures in each passband at Kitt Peak at zenith distances of ~60°. The dotted lines in Figure 1 connect these two points, assuming a linear dependence on air mass, which is roughly correct. One should be cautious when comparing sky brightness measurements for different sites, because of the strong variability over time visible in these figures, especially in a case like Mount Hopkins/Kitt Peak, where we have no information on long-term variations. An additional source of uncertainty arises because Massey & Foltz (2000) derived their broadband sky brightness values from spectrophotometry, replacing the variable [O I] λ5577 line with an average value. Nonetheless, we can see that several VATT observing runs had sky surface brightness values that were significantly darker than the Mount Hopkins/Kitt Peak numbers given by Massey & Foltz (2000), who point out that their numbers are comparable to those from Palomar Observatory in the early 1970s, which was considered a rather dark site at the time.

Figure 3 shows the median sky surface brightness at the VATT, per observing run, of all low air mass (sec $z$ < 1.2) stacked galaxy images taken during photometric conditions, as a function of time. One obvious outlying sky brightness value from the 2002 January run in *U* and *B* was rejected, since it was measured near morning twilight and therefore contaminated our results. For comparison, we overlay the average values from Mount Hopkins/Kitt Peak (Massey & Foltz 2000),

TABLE 1
AVERAGE PHOTOMETRIC SKY SURFACE BRIGHTNESS ($\mu$) NEAR ZENITH AT VARIOUS SITES

| Site | Condition | Observation Dates | $\mu_U$ | $\mu_B$ | $\mu_V$ | $\mu_R$ |
|---|---|---|---|---|---|---|
| Mount Graham[a] ...... | Darkest run | *U*: 2000 Feb, *BVR*: 2001 Feb | 22.38 | 22.86 | 21.72 | 21.19 |
| | All runs | 1999 Apr–2002 Apr | 22.00 | 22.53 | 21.49 | 20.88 |
| | Brightest run | 1999 Apr | 21.68 | 22.01 | 21.04 | 20.46 |
| Mount Hopkins[b] ...... | ... | 1998 Nov | ... | 22.63 | 21.46 | ... |
| Kitt Peak[b] ............ | ... | 1999 Nov | ... | 22.63 | 21.44 | ... |
| Mauna Kea[c] .......... | Solar minimum | 1996 | ... | 22.84 | 21.91 | ... |
| | Solar maximum | 1992 | ... | 22.22 | 21.29 | ... |
| La Palma[d] ............ | ... | 1987–1996 | 22.0 | 22.7 | 21.9 | 21.0 |
| ESO/La Silla[e] ......... | ... | 2000 Apr–2001 Sep | 22.3 | 22.6 | 21.6 | 20.9 |
| Cerro Tololo[f] ......... | ... | 1987–1988 | 22.0 | 22.7 | 21.8 | 20.9 |
| Cerro Tololo[g] ......... | ... | 1997 | ... | 22.7 | 22.0 | ... |

NOTE.—All sky surface brightness values have units of mag arcsec$^{-2}$.
[a] Mean error on mean Mount Graham values $\lesssim$0.04 mag arcsec$^{-2}$.
[b] Massey & Foltz (2000). Calculated from spectrophotometry.
[c] Krisciunas (1997).
[d] Benn & Ellison (1998). Solar minimum and high Galactic and ecliptic latitude. Measured 0.4 mag arcsec$^{-2}$ brighter at solar maximum.
[e] Patat (2003). Values corrected to zenith.
[f] Walker (1987) and Walker & Schwarz 1987–1988 (see footnote 2).
[g] Walker & Schwarz 1987–1988 (see footnote 2).

Cerro Tololo (Walker 1987; Walker & Schwarz 1987–1988[2]), and La Palma (Benn & Ellison 1998). Again, we caution against putting strong confidence in such comparisons, for the reasons previously mentioned. On occasion the VATT was darker than Cerro Tololo, except in the *V* band. The La Palma observations were made from 1987 to 1996, and the values plotted in Figure 3 are the solar minimum values given by Benn & Ellison (1998) minus the quoted 0.4 mag difference between solar minimum and maximum, since our data was taken near solar maximum. For the most part, our values are consistently darker than La Palma's solar maximum skies, and similar to La Palma solar minimum skies (sometimes brighter, sometimes darker, although always brighter in the *V* band). Figure 3 clearly shows a strong variability of several tenths of a magnitude in sky brightness from observing run to observing run, with a general brightening of the sky toward solar maximum (2000–2002). The anomalously bright point during solar minimum in 1999 may have been due to smoke from nearby forest fires.

In Table 1 we list for comparison our average photometric low air mass sky surface brightness values for the VATT, Mount Graham, and for various other sites. We also give sky surface brightness values for our darkest and brightest runs. Excluding the Mauna Kea solar maximum values (Krisciunas 1997), which are significantly brighter than any of the measurements for the other sites, the darkest *B*-band sky surface brightness at sites other than Mount Graham range from 22.6 to 22.84 mag arcsec$^{-2}$, compared to our average value of 22.53 mag arcsec$^{-2}$. Our darkest run was 22.86 mag arcsec$^{-2}$, which is marginally darker by 0.02 mag arcsec$^{-2}$ than the darkest site (Mauna Kea at solar minimum). Since our observations were made near solar maximum, we can expect the Mount Graham site to become darker still during periods of low solar activity in 2006–2007. Sites other than Mount Graham had *V*-band sky brightness values that varied between 21.44 and 22.29 mag arcsec$^{-2}$, compared to the Mount Graham average of 21.49 mag arcsec$^{-2}$. Our darkest run had a *V*-band sky surface brightness of 21.72 mag arcsec$^{-2}$, which is 0.28 mag arcsec$^{-2}$ darker than the brightest site (Kitt Peak; Massey & Foltz 2000) and 0.28 mag arcsec$^{-2}$ brighter than the darkest site (CTIO during solar minimum; Walker & Schwarz 1987–1988 [see footnote 2]), although again, our observations were at solar maximum. There are fewer published sky surface brightness values in *U* and *R*, but in the cases in which we can make a comparison (La Palma, Benn & Ellison 1998; ESO, Patat 2003; and Cerro Tololo, Walker 1987), our Mount Graham averages are similar, and our darkest run was 0.08 mag arcsec$^{-2}$ darker in *U* than ESO, and 0.19 mag arcsec$^{-2}$ darker in *R* than La Palma.

We can compare our measured sky brightness values to the Garstang (1989) predicted *V*- and *B*-band sky surface brightness values for Mount Graham. Garstang calculated *V*-band sky brightness values for very clear air, during solar minimum, and using 1980 populations for nearby towns and cities. This resulted in a predicted MGIO *V*-band sky brightness of 21.94 mag arcsec$^{-2}$ at the zenith, and 21.72 mag arcsec$^{-2}$ at a zenith distance ($z$) of 45°. This agrees well with our darkest run, which had an average *V*-band sky surface brightness of 21.72 $\pm$ 0.04 mag arcsec$^{-2}$ for $z \lesssim 33\overset{\circ}{.}6$. Our measured value is slightly brighter than what would be expected from Garstang's predictions, but this can easily be explained by an increase in population since 1980 and the fact that our mea-

[2] See http://www.ctio.noao.edu/site/pachon_sky.

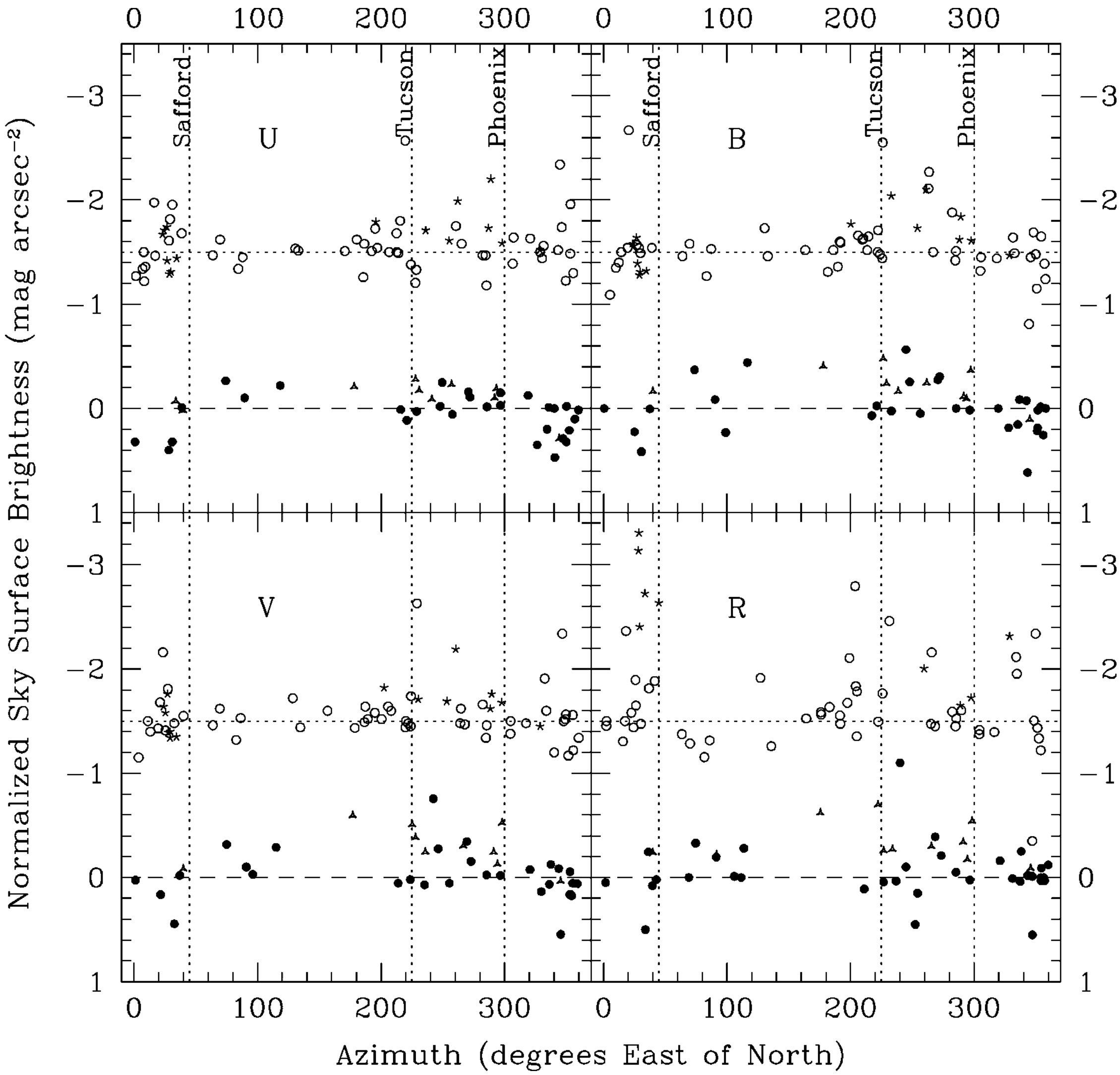


FIG. 4.—Sky brightness normalized to the median sky for the observing run, where $\sec z \le 1.3$ and Moon illumination ≤20°. Nonphotometric points (*open circles for* $20° \le z < 40°$, *asterisks for* $z \ge 40°$) are arbitrarily offset from photometric points (*filled circles for* $20° \le z < 40°$, *triangles for* $z \ge 40°$). The normalized median is marked with a dotted (nonphotometric) or dashed (photometric) horizontal line. Vertical dotted lines mark the general direction of three cities that might affect the sky brightness.

surements were taken near solar maximum. Garstang also predicted *B*-band sky surface brightness values of 22.93 mag arcsec$^{-2}$ at $z = 0°$ and 22.75 mag arcsec$^{-2}$ at $z = 45°$, which agrees well with our darkest run, which had an average *B*-band sky surface brightness of 22.86 mag arcsec$^{-2}$ for $z \lesssim 33.6°$.

To determine how nearby city lights affect sky brightness, we plot sky surface brightness versus the azimuth (az) of our observations (Fig. 4). Data taken during nights on which Moon illumination was ≥20% were rejected from this plot. We normalized the sky brightness of each image to the median sky surface brightness for the $\sec z \le 1.3$ data in each observing run, and arbitrarily offset data points taken during nonphotometric conditions from those taken during photometric nights. Open circles (nonphotometric) and filled circles (photometric) represent images taken at mid-zenith distances ($20° \le z < 40°$), while asterisks (nonphotometric) and triangles (photometric) represent images taken at high-zenith distances ($z \ge 40°$). Vertical dotted lines mark the general direction of three cities that may potentially contribute to light pollution at the Mount Graham site.

Figure 4 shows that images observed toward the North during photometric conditions tend to have darker skies than all other directions. Darker northern skies are seen to a lesser extent with increasing wavelength (0.2, 0.1, 0.06, and 0.00 mag arcsec$^{-2}$ darker than the median sky in *U*, *B*, *V*, and *R*, respectively) and not at all in the nonphotometric data (due to the presence of cirrus). This implies that the effect may be due more to the large angular distance of these pointings from the zodiacal belt and the Milky Way than to the absence of city lights in that direction. Phoenix and Tucson contribute somewhat to sky brightness, with photometric skies between the two cities ($220° < \mathrm{az} < 300°$) that are brighter than the median sky by 0.1 mag arcsec$^{-2}$ in *U* and 0.2 mag arcsec$^{-2}$ in *BVR*. This brightening toward Tucson and Phoenix is strongest at high-zenith distances ($z \geq 40°$) and during nonphotometric conditions, which is consistent with the expected reflection of city lights off of clouds or cirrus. Safford has less of an effect on sky brightness, however, with no measurable brightening in that direction during photometric conditions. The only exception is in the *R* band during nonphotometric conditions, where the sky in that direction is 0.4 mag arcsec$^{-2}$ brighter than the median. This might be due at least in part to sodium lamps from Safford, which emit at 5500–6500 Å and are therefore most apparent in *R* ($\lambda_e \sim 6340$ Å). This is consistent with Massey & Foltz (2000), who estimated the contribution of such lamps in Tucson to be 0.17 mag arcsec$^{-2}$ at the zenith of Kitt Peak and Mount Hopkins, with a larger effect expected at higher zenith distances and with the presence of clouds. Our brightest sky measurements toward Safford are outlying nonphotometric, high air mass data points, and so overall, Safford contributes very little to the night-sky brightness at the location of the VATT on Mount Graham. Garstang (1989) predicted that the night sky would be brightest toward Safford at a modest zenith distance of 45°, and considerably brighter toward Tucson than any other direction at the extreme zenith distance of 85°. However, Tucson affects our sky brightness measurements more than Safford in almost all cases. This is in part because the Safford lights are shielded by the mountain peak at the VATT's location, and also because of the strict dark-sky ordinances in place in Safford, as well as faster growth in Tucson than Safford since Garstang's 1980 population calculations. Also, smog carried up from the Tucson Valley to the nightly inversion layer likely reflects the city lights better than the clean air above Safford. Overall, city lights have little affect on the sky brightness at Mount Graham, making it a prime dark-sky site.

Sky brightness can also vary with time of night, as addressed by Walker (1988), who found an exponential decrease of 0.4 mag in *B* and *V* during the first half of the night at San Benito Mountain. Since this decrease was observed near the zenith and was independent of overall sky brightness, time of year, and the presence of fog, Walker concluded that it is more likely due to a natural phenomenon than a decrease in the contribution of city lights throughout the night. Walker mentions that this may be partially due to a decrease in the zodiacal light contribution throughout the night, but is likely primarily due to the recombination of ions that were excited during the day by solar EUV radiation.

We investigate this trend at Mount Graham in Figure 5, which shows the dependence of sky surface brightness in *UBVR* on the fraction of the night in which the beginning and end of the night in each run is defined as the end and beginning of astronomical twilight for the midpoint of that run. We plot only data points taken during moon illumination of ≤20% and at $z \leq 40°$. We normalized the sky brightness of each image to the median sky surface brightness for the $\sec z \leq 1.3$ data in each observing run, and arbitrarily offset data points taken during nonphotometric conditions from those taken during photometric nights by 1.5 mag. We approximate the nightly sky brightness trend with a linear least-squares fit that does not include measurements taken within 0.5 hr of twilight (*solid lines*). The *UB* photometric data show no significant trend with time of night. There is, however, a trend in photometric data in *V* and *R* (which is expected, due to the nightly decrease in [O I] λ5577 and λλ6300–6334 emission line strengths), with a decrease in the first half of the night of 0.1 mag arcsec$^{-2}$ in *V* and 0.2 mag arcsec$^{-2}$ in *R*, followed by a slight increase in sky brightness toward the very end of the night. This is less than the 0.4 mag arcsec$^{-2}$ decrease seen in *B* and *V* by Walker (1988), which may be a result of the difference in elevation of Mount Graham (10,400 feet [3170 m]) and San Benito Mountain (5248 feet [1600 m]). This highlights one of the advantages of Mount Graham's high elevation, which contributes in many ways to make it a particularly dark site. Nonphotometric data show a stronger trend, with an overall decrease in sky brightness of 0.2, 0.3, 0.3, and 0.4 mag arcsec$^{-2}$ throughout the night in *U*, *B*, *V*, and *R*, respectively. The reason for this decrease in sky brightness is uncertain at this time, but it may be related to a general decrease of cloud cover throughout the night, which we often recorded in the observing logs. Local humidity-driven weather induced by Mount Graham itself may be responsible for this, especially in late spring to early fall, when the humidity is higher.

## 4. TRENDS IN ESTIMATED SEEING OR STELLAR FWHM AT THE VATT

### 4.1. Measuring the Stellar FWHM

The FWHM of stars measured with the VATT 2K CCD is affected by telescope focus, in addition to atmospheric effects. The actual focus value depends on several factors, such as optics, temperature, air mass, and filter. Since the VATT has a fast ∼f/1 primary mirror, its focus is very sensitive to changes in temperature during the night. Once the telescope has reached equilibrium with the night air, the automated telescope software adjusts the focus to account for temperature and air mass changes. However, it is frequently necessary for the observer to refocus the telescope as the temperature drops, particularly at the start of each night. Also, as the focus changes throughout the night, the FWHM may deteriorate progressively over time, which raises the average stellar FWHM values with respect to the actual atmospheric seeing. Consistently rechecking the focus throughout the night can minimize this effect. Since these data were taken as part of a galaxy survey that focuses mainly on *U*-band galaxy surface photometry, we typically only focused in *U*. The change in focus between filters is small, since

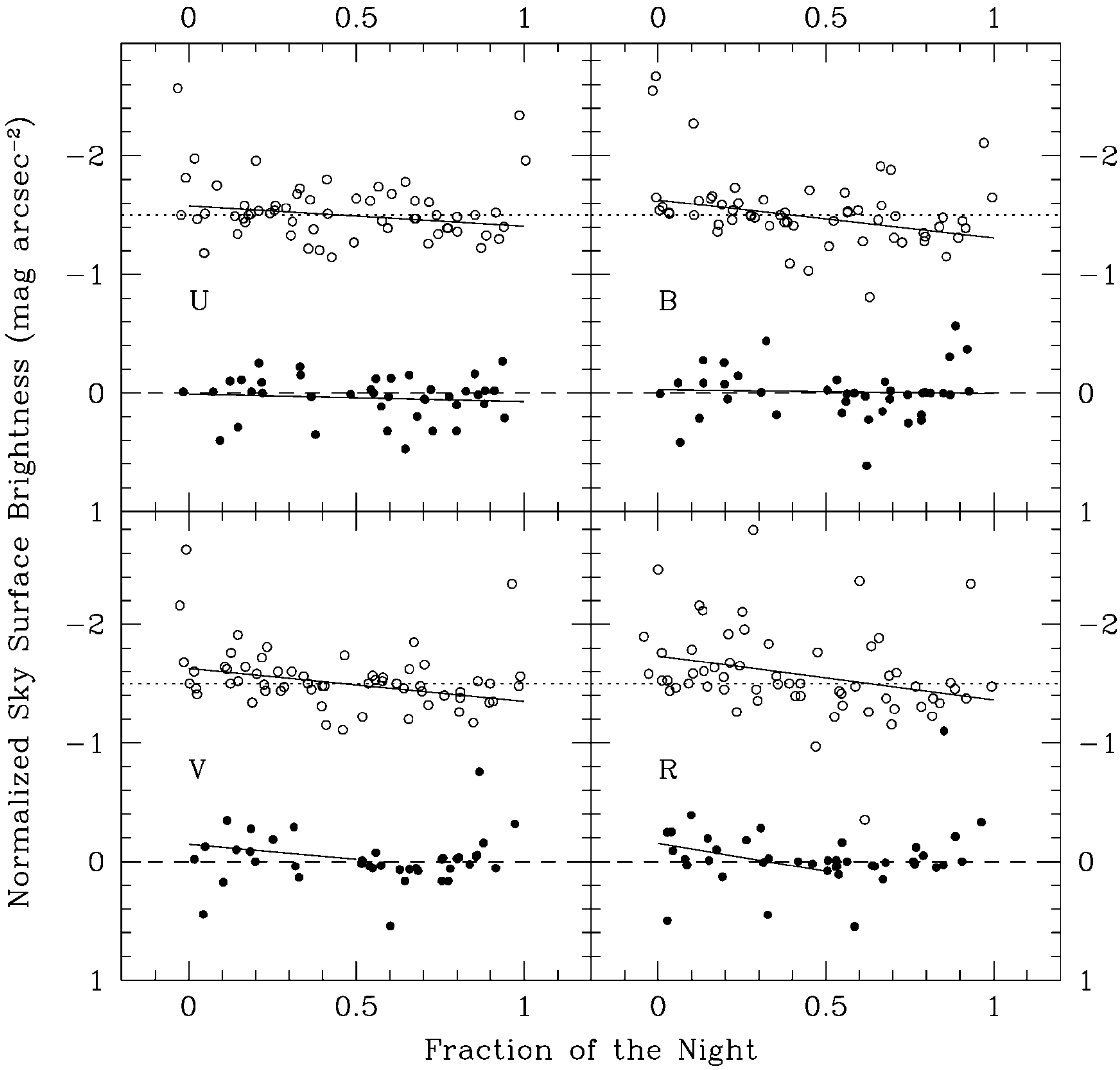


FIG. 5.—Sky brightness normalized to the median sky for the observing run, where sec $z \leq 1.3$ and Moon illumination ≤20°. Nonphotometric points (*open circles*) are arbitrarily offset from photometric points (*filled circles*). The normalized median is marked with a dotted (nonphotometric) or dashed (photometric) line. The beginning and end of the night is defined by the end and beginning of astronomical twilight for the midpoint of the observing run such that dusk is at fraction = 0 and dawn is at fraction = 1. Solid lines are the linear least-squares fits to the data, excluding measurements taken within 0.5 hr of twilight.

all of the filters are nearly par-focal, but focusing only in *U* may have resulted in a slightly larger average seeing value in *B*, *V*, and *R* than could have been obtained if the images had been focused in each filter separately. Therefore, we offer a cautionary note that the FWHM values in our galaxy images are likely to be larger than what we could achieve at the VATT, had each of them been focused in their particular target filter, and if each galaxy image had been preceded by a focus check. Also, since the FWHMs from the galaxy images presented in this paper were measured from stacked images, they will be marginally larger than if we had measured them from the individual images. This is due to small errors in image alignment from the applied integer shifts.

We measured the stellar FWHM for all of our stacked galaxy images using the LMORPHO package (Odewahn et al. 2002), which imports a list of all sources and their FWHMs produced with SExtractor (Bertin & Arnouts 1996). Stars are selected from the source list for each image by interactively defining limits on a plot of FWHMs versus magnitude, like the one shown in Figure 6. As can be seen in this plot, the FWHM of stars does not significantly depend on their brightness (except for bright saturated stars), while brighter galaxies tend to be larger in size, creating a quick way of identifying stars. This semiautomated method works well for most galaxy images, although problems may occur for fields that contain very few bright stars. In such cases, our seeing estimate may be too

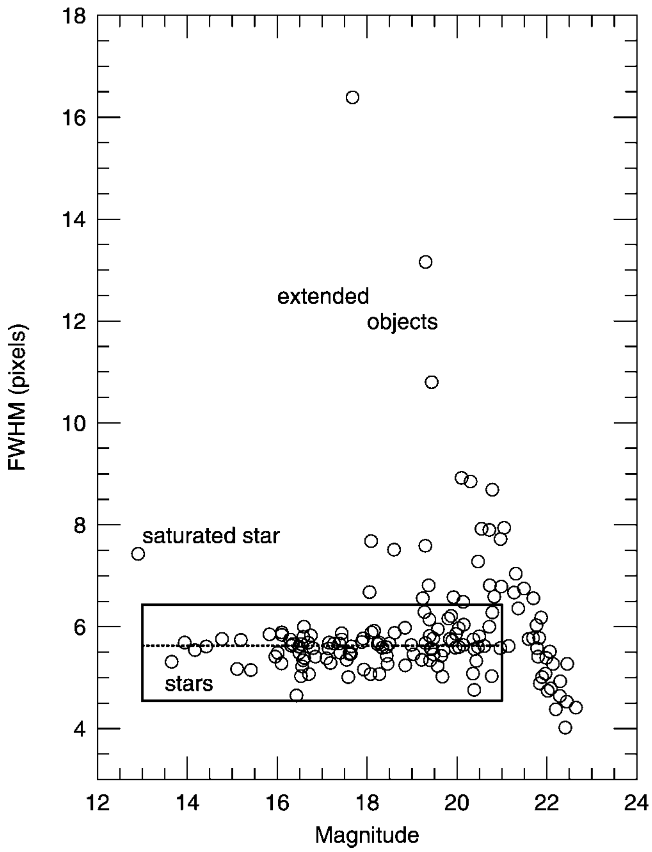


FIG. 6.—Object FWHMs vs. apparent magnitude in a single galaxy field. We use the fact that the FWHM of a star does not depend on its brightness to separate stars and extended objects, as labeled on the plot. For the purpose of our semiautomated seeing measurements, we excluded saturated stars and those that are too faint to yield reliable measurements. The filled box encloses the objects that were used to compute the mean stellar FWHM for this field (*dotted horizontal line*).

large, since the star selection may be contaminated by some faint extended objects.

In order to obtain more accurate measurements of atmospheric seeing than is possible with galaxy images, we also measure the FWHM of the stars with the best focus in our focus exposures, using IMEXAM within IRAF.[3] These focus exposures are single images in which five to seven short exposures at different focus settings are recorded, and prior to each exposure, the charge on the CCD is shifted by 50–100 pixels. Because these exposures are short, the stellar images are not affected by tracking and guiding errors or by telescope vibrations (as we will show below, this was particularly problematic in our earlier runs). Independent FWHM measurements by two of us (V. T. and R. J.) agree to within the measurement errors (typically ∼0″.05–0″.10).

[3] IRAF is distributed by the National Optical Astronomy Observatories, which are operated by the Association of Universities for Research in Astronomy, Inc., under cooperative agreement with the National Science Foundation.

### 4.2. Estimated Seeing Results

Figure 7 shows the median FWHM of stars measured in our stacked galaxy images as a function of air mass in *UBVR*; it is split into separate panels for each observing run. There is a clear trend of increasing FWHM with air mass, which is to be expected from the theoretical relation[4]

$$\mathrm{FWHM}(z) = \mathrm{FWHM}(0)\sec(z)^{0.6}, \qquad (2)$$

but like the sky surface brightness, this trend does not seem to have a particularly consistent slope from one run to the next (possibly because the automatic focus did not correct for air mass dependence accurately enough). Stacked images that are composed solely of individual images taken during photometric conditions (with $\lesssim 3\%$ variation in magnitude zero point throughout the night) are plotted as asterisks, while those composed of images taken during nonphotometric conditions are plotted as open circles. This reveals that there does not seem to be a clear trend of seeing with photometricity. However, we note that in the two runs in which there is a significant difference between the seeing on the photometric and nonphotometric nights (1999 April and 2000 May), the nonphotometric nights had better seeing. The observation log sheets noted the presence of cirrus, which is often correlated with stable air and better seeing. Filled squares in this plot represent the FWHM of the stars with the best focus in the short-focus exposures. These FWHM values tend to be smaller than or equal to the stellar FWHM measured in galaxy images taken immediately after the focus exposures, for the reasons mentioned in the previous section. As the telescope focus degrades with time between focus exposures, the stellar FWHM in the galaxy images will increase. Thus, the focus FWHM values are indeed a more accurate measurement of the atmospheric seeing.

Figure 8 shows the median low air mass ($\sec z < 1.2$) FWHM values for each run, with filled circles representing the stellar FWHM in the stacked galaxy images, and open circles representing the best focus FWHM in the focus exposures. In almost all cases, the median FWHM in the focus exposures are smaller than those in the galaxy images, as expected. Except for the 2001 February observing run, which had particularly good seeing, it is apparent that the average FWHM values and their uncertainties (which reflect the range of the data) are much larger for the runs before 2001 May. This change in FWHM values corresponds to an engineering run in summer 2001, during which a vibration in the secondary mirror mount that had contributed up to 0″.4 to the FWHM was removed (M. Nelson 2003, private communication). Adjustments were also

[4] See http://www.ing.iac.es/Astronomy/development/hap/dimm.html.

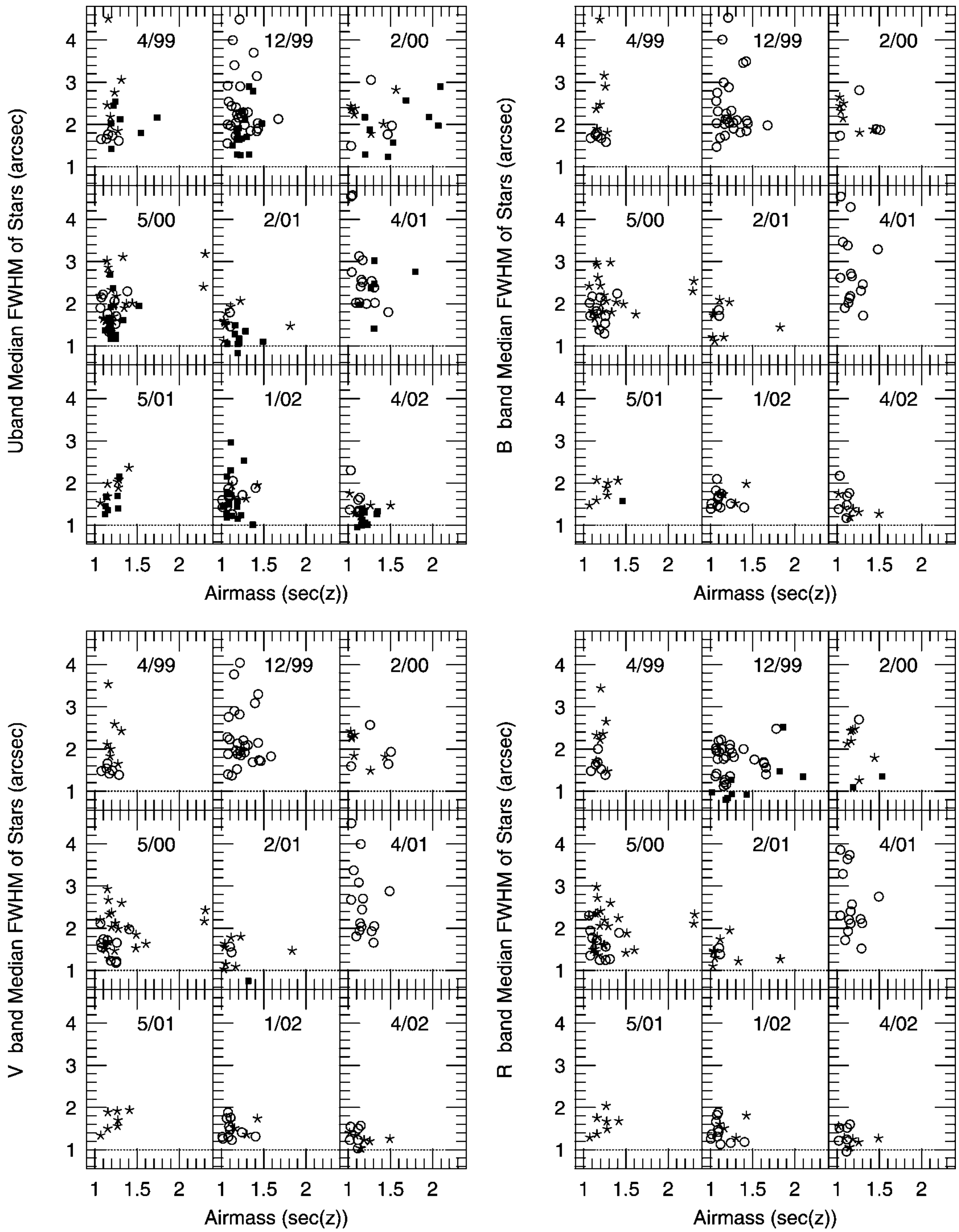


FIG. 7.—Median stellar FWHM in images taken at the VATT between 1999 April and 2002 April in *U*, *B*, *V*, and *R*. Each of our observing runs is indicated in a separate subpanel. Measurements obtained under nonphotometric conditions are represented by open circles, while measurements from photometric nights (zero-point variations of ≲3% throughout the night) are indicated by asterisks. The filled squares represent the stellar FWHM corresponding to the best focus setting as measured in short-focus exposures. These tend to be smaller than or equal to the FWHMs measured in adjacent object exposures. We typically focused the telescope in *U*, since that is where most of our galaxy images would be taken.

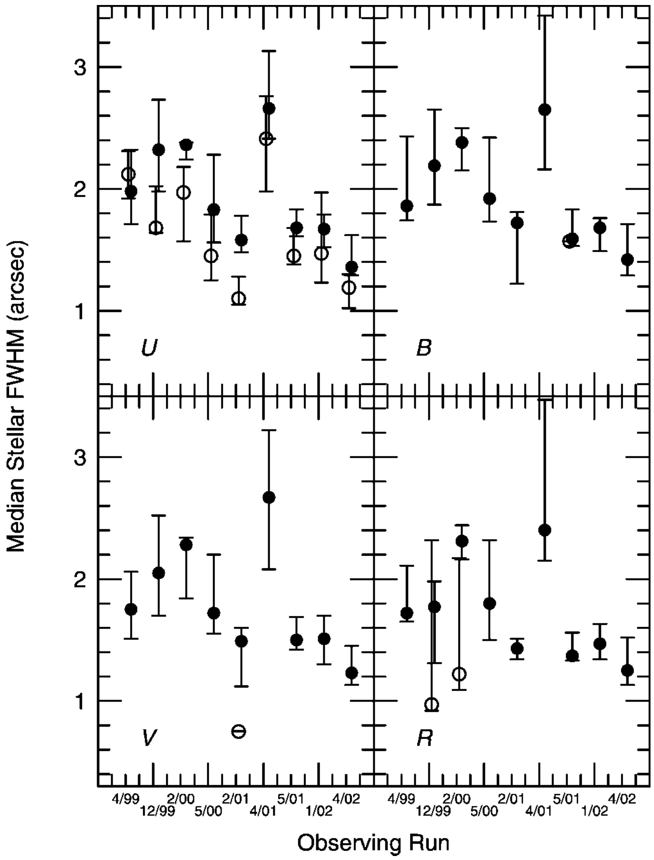


FIG. 8.—Historical trend in our FWHM measurements. *Filled circles*: Median stellar FWHM at low air mass (sec $z < 1.2$), measured in our stacked galaxy images. *Open circles*: Median FWHM of the best focus setting, measured in short-focus exposures. Error bars represent the 25%–75% quartile range for each run. Improvements to the telescope in summer and fall 2001 significantly reduced the stellar FWHMs measured during the later runs.

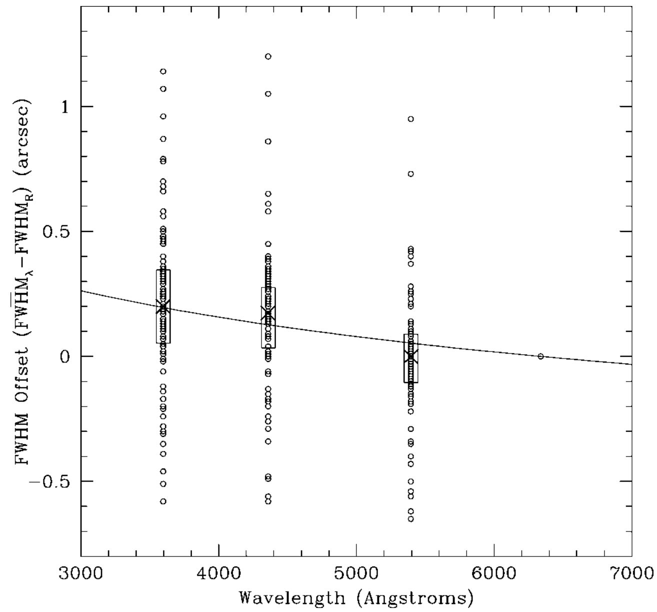


FIG. 9.—*Open circles*: Stellar FWHM of each stacked galaxy image, minus the stellar FWHM in the *R*-band image of that galaxy, producing a measure of the FWHM offset between filters at the VATT. Outliers are due to highly variable seeing conditions or cases in which a focus exposure was taken between observations for a single galaxy. Galaxies for which observations in each filter were not carried out immediately after one another are not included on this plot. *Crosses*: Median FWHM$_\lambda$–FWHM$_R$ offset from theory for each filter. The boxes surrounding the medians enclose the 25%–75% quartile range. *Solid line*: Value the offsets would have if the FWHMs followed the theoretical $\lambda^{-1/5}$ dependence, using the median FWHM$_R$ value of 1″.63. The divergence of theory from the median observed offsets are due to specific telescope properties at the VATT that cause a systematic contribution from the telescope to the wavelength dependence of the seeing. The scatter in this plot gives random offsets from theory that are partially due to atmospheric variations and partly due to telescope vibrations (which is particularly important for the earlier runs). This vibrational component cannot be separated from the atmospheric effects, but it cannot be larger than the standard deviation of the points, which is $\simeq$0″.2 in all filters.

made to the pointing map in fall 2001. As Figure 8 shows, both of these improvements resulted in a significant reduction of the FWHM of the VATT PSF. Table 2 lists the average of the median stellar FWHM values in the galaxy images for all runs (ignoring the outlying 2001 April run) before and after the improvements. There was an overall improved seeing of about 0″.45 in all filters, as well as a more stable focus, as can be seen in the decreased FWHM scatter between these two time periods in Figure 7, and in the smaller uncertainties in Figure 8 and Table 2. After the improvements, we were able to obtain subarcsecond seeing in one of our combined images in *R* in 2002 April (see Fig. 7), even though we focused in a different filter, and we routinely measured subarcsecond seeing in the focus frames.

The stellar FWHM values from the galaxy images are useful in determining the average FWHM that one might realistically achieve in long (3–20 minute) object exposures at the VATT, with better results possible with more frequent focusing and with refocusing done for each filter. However, the best FWHM values are obtained through the shorter focus (several second) exposures.

We can compare the FWHM in focus exposures taken in different filters by determining the offset in the PSF between filters, which is a result of both the wavelength dependence of atmospheric seeing and the contribution of the telescope. Atmospheric seeing has been studied extensively in the past (e.g., Kolmogorov 1941; Tatarski 1961; and Fried 1965), and has been reviewed and summarized more recently by Coulman (1985) and Roddier (1981). The Fried parameter $r_0$ is a measure of the average effective size at a given wavelength $\lambda$ of the elements of air that are responsible for the angular deviations of light from a distant point source, which is the cause of atmospheric seeing. Where $r_0 \propto \lambda^{6/5}$, the FWHM measured in seeing estimates is related to $r_0$ by

$$\mathrm{FWHM} = 0.98\,\lambda\, r_0^{-1}, \qquad (3)$$

TABLE 2
MEDIAN STELLAR FWHM MEASUREMENTS AT THE VATT

| Type | Date | $U$ (arcsec) | $B$ (arcsec) | $V$ (arcsec) | $R$ (arcsec) |
|---|---|---|---|---|---|
| Best median focus[a] | 2001 Feb, 2002 Oct | … | … | … | 0.97 ± 0.06 |
| Worst median focus[a] | 2001 Apr | … | … | … | 2.15 ± 0.42 |
| Best FWHM in single-focus exposure[a] | 2001 Feb | … | … | … | 0.65 |
| All galaxy images[b] | 1999 Apr–2001 Feb | 2.01 ± 0.25 | 2.01 ± 0.34 | 1.86 ± 0.39 | 1.81 ± 0.24 |
| All galaxy images[c] | 2001 May–2002 Apr | 1.57 ± 0.10 | 1.56 ± 0.12 | 1.41 ± 0.12 | 1.36 ± 0.08 |
| Best median in galaxy images[d] | 2002 Apr | 1.36 ± 0.03 | 1.42 ± 0.06 | 1.23 ± 0.04 | 1.25 ± 0.05 |
| Worst median in galaxy images[d] | 2001 Apr | 2.66 ± 0.12 | 2.65 ± 0.22 | 2.67 ± 0.26 | 2.40 ± 0.11 |
| Best FWHM in single galaxy image | *UBV*: Feb 2001, *VR*: Apr 2002 | 1.12 | 1.12 | 1.03 | 0.95 |

NOTE.—Stellar FWHM values measured in focus frames are closer to the true atmospheric seeing than stellar FWHM values measured in galaxy images, because focus exposures are short (a few seconds, compared to a few minutes) and record the best telescope focus (which may have deteriorated in galaxy exposures). Focusing must be done frequently (at least once an hour, possibly more at the beginning of the night and less toward the end of the night) in order to obtain the best stellar FWHM values in deep-object exposures. For our galaxy images, we typically focused in $U$. Focusing in each filter separately would result in smaller stellar FWHMs in the other passbands.

[a] Exposures taken in filters other than $R$ were reduced to $R$ using the theoretical $\lambda^{-1/5}$ dependence and the observed contribution from the telescope added in quadrature. Median values are per observing run.

[b] Before telescope improvements in summer and fall 2001.

[c] After telescope improvements in summer and fall 2001.

[d] Median values are per observing run.

which results in a $\lambda^{-1/5}$ dependence of the FWHM on wavelength. To test this relation and find the FWHM contribution from the telescope, we plot the stellar FWHM of our images in each filter, minus the stellar FWHM for that field in the $R$ band (Fig. 9). We only include galaxies where exposures in each filter were taken immediately after one another, in order to limit the effects of air mass and large-scale seeing changes between exposures during the night. The outlying points were likely due to fields that were imaged during highly variable seeing conditions or which had focus exposures taken between observations. The solid curve in Figure 9 traces the theoretical $\lambda^{-1/5}$ FWHM dependence, while the crosses mark the median $\mathrm{FWHM}_\lambda$–$\mathrm{FWHM}_R$ offset from the $\lambda^{-1/5}$ relation. The slight offset between the observational medians and the theoretical $\lambda^{-1/5}$ line gives the systematic contribution of the telescope to the wavelength dependence of the stellar FWHM. The scatter in this plot gives a measure of the random contribution of the atmosphere and telescope to the wavelength dependence, which can be due to both atmospheric variations and telescope vibrations (which is more important for the earlier runs, before the telescope improvements made in summer and fall 2001). These factors cannot be separated from one another in this plot, but we can put an upper limit on the random contribution from the telescope, which would be the standard deviation in the points, divided by $\sqrt{2}$ (since the errors in the target filter plus those in $R$ combine in quadrature), which is $\simeq 0\farcs1$ in all filters.

In order to more carefully determine the telescope contribution to the wavelength dependence of the seeing, we plot the offsets between observation and the $\lambda^{-1/5}$ relation as a function of FWHM as measured in $R$ in Figure 10. Points with offsets from theory greater than $0\farcs3$, which is significantly larger than the standard deviation of about $0\farcs2$, are rejected in order to exclude outliers caused by variable atmospheric seeing. Visual inspection of these plots reveal that the telescope's contribution to the wavelength dependence of stellar FWHM has no clear dependence on FWHM, which suggests a constant offset for all cases. The median $\mathrm{FWHM}_\lambda$–$\mathrm{FWHM}_R$ offsets from theory found in this graph ($0\farcs006$ for $\lambda = U$, $0\farcs055$ for $\lambda = B$, and $-0\farcs050$ for $\lambda = V$) provide a measure of the telescope contribution to the FWHM wavelength dependence, which is small and is well within the standard deviation of the observed FWHMs for all images. This telescope contribution, plus the atmospheric contribution given by the $\lambda^{-1/5}$ relation, have been applied to the FWHM in each filter to reduce it to the FWHM that would have been measured in an $R$-band exposure adjacent in time in Figure 11.

Figure 11 shows a plot of all focus FWHM values in our nine 1999 April to 2002 April observing runs, plus focus FWHM values for eight additional observing runs conducted by one of us (R. J.) for other projects spanning 2001 November to 2003 December. All values have been reduced to the $R$ band using the $\lambda^{-1/5}$ theoretical relation, plus the observational telescope offsets from theory found in Figure 10. The nine 1999 April to 2002 April runs have values that are consistent with the eight 2001 November to 2003 December runs, even though each data set was observed and analyzed independently. The additional runs give us better statistics for more recent years and thus verify that the observing runs before the telescope improvements (those to the left of the dotted line, which marks the end of the improvements in 2001 October) have overall worse stellar FWHM values and larger scatter than those after the telescope improvements. The observing run with the worst individual FWHM measurements was noted as having strong winds from the northeast, which is well known to cause bad atmospheric seeing conditions at the VATT. Under the best conditions, we were able to measure subarcsecond seeing for

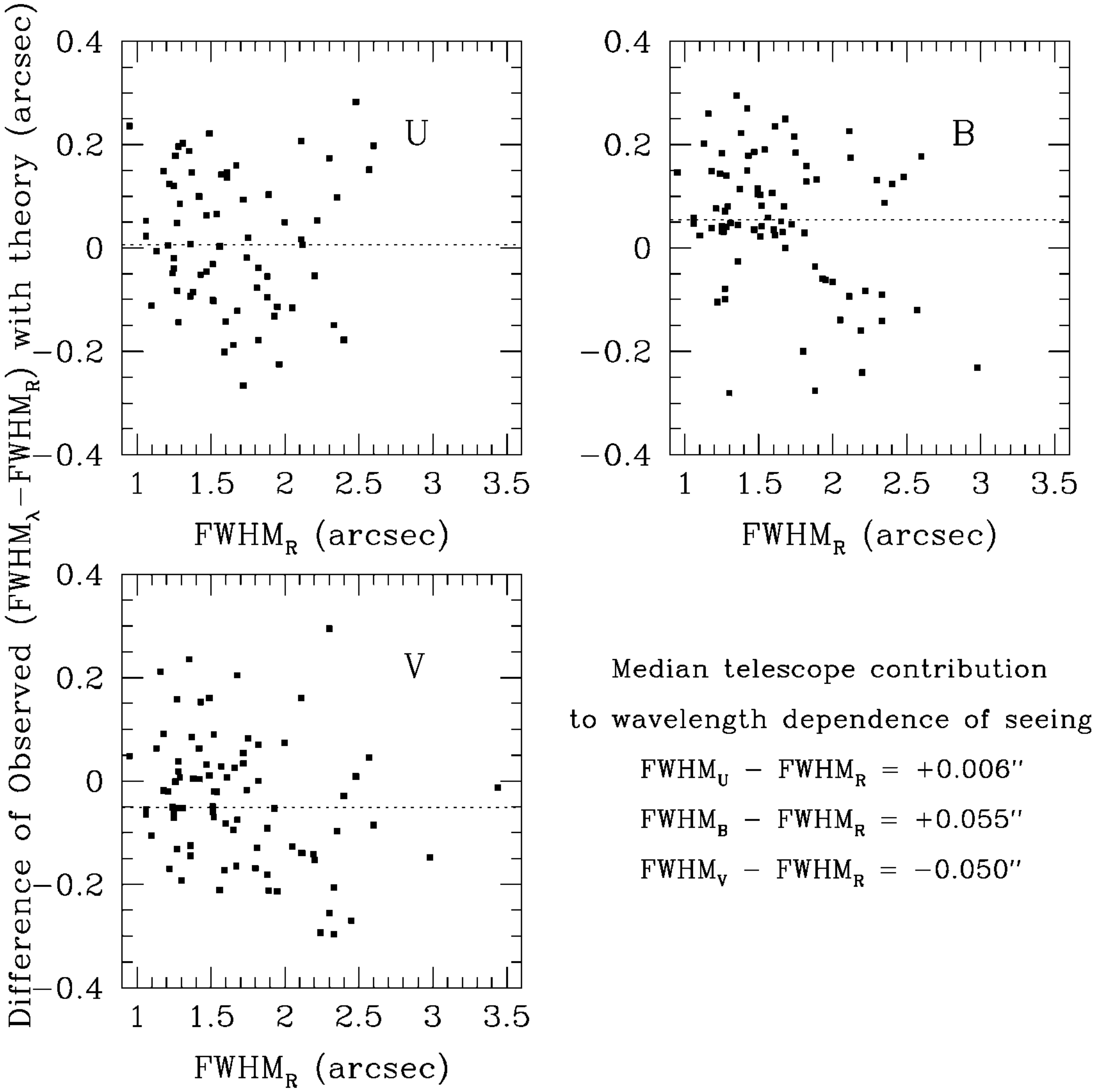


FIG. 10.—Comparison of the theoretical $\lambda^{-1/5}$ wavelength dependence of stellar FWHM to the observed wavelength dependence for each image, for the purpose of reducing FWHM values to the *R* band in order to compare focus exposures taken in different filters (as in Fig. 11). We find the observed FWHM in each passband (*UBV*), minus the FWHM in the reference filter *R*, and subtract this from the theoretical result, then plot this offset versus the observed FWHM in *R*. Galaxies for which observations in each filter were not carried out immediately after one another are not included. Points with offsets from theory greater than 0″.3 (which is outside the standard deviation of 0″.2 for all of the points) were rejected to avoid outliers caused by variable atmospheric conditions. There is no strong dependence on $FWHM_R$ for this offset in any filter, and thus we apply a constant small-telescope correction to all FWHM values in Fig. 11 of the median (observation minus theory) offset in *UBV* (*listed in the figure and marked by dotted lines*), plus the atmospheric contribution given by the $\lambda^{-1/5}$ relation.

many of the focus exposures, especially after the telescope improvements in summer and fall 2001.

Table 2 summarizes the stellar FWHMs in the galaxy images and the focus exposures. Median stellar FWHM values range from 0″.97 to 2″.15 in *R* focus exposures, and 1″.25 to 2″.40 in *R* galaxy images. The best stellar FWHM measured was 0″.65 in an *R* focus exposure, and 0″.95 in an *R* galaxy image. This amounts to a linear increase in FWHM of 0″.25–0″.30 in long exposures, which is partially due to vibrations and variable atmospheric seeing, and partially due to the fact that galaxy images may not have been taken at the best telescope focus. Different values could be measured at other telescope sites on Mount Graham, since there may be a significant telescope contribution to these values, and also because dome-high trees that surround the VATT site negatively impact the seeing.

## 5. CONCLUSIONS

Figures 1 and 3 and Table 1 suggest that Mount Graham has an average sky brightness that is similar to other dark sites and can occasionally have darker skies than some of the sites reviewed here. We have found that sky brightness is highly var-

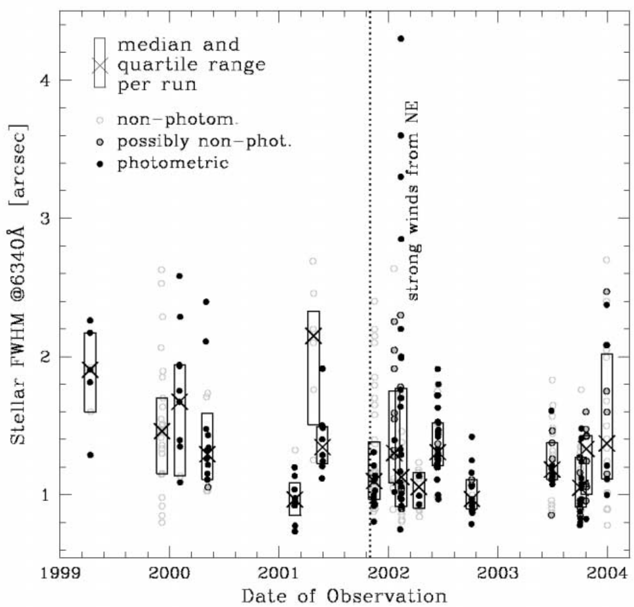


FIG. 11.—VATT focus exposure stellar FWHM values normalized to the $R$ band using the theoretical atmospheric $\lambda^{-1/5}$ dependence, plus the observational median telescope contribution offsets found in Fig. 10. This plot includes observing runs carried out by one of us (R. J.), in addition to the observing runs the rest of this paper focuses on. The worst FWHM values were measured when strong winds were blowing from the northeast, which always results in particularly bad seeing conditions at the VATT. Subarcsecond $R$-band seeing was reached on occasion throughout this time period. FWHM values are highly variable, although an overall improvement in median FWHM and scatter is apparent in the observing runs following telescope improvements made in summer and fall 2001. The dotted line marks the end of the implementation of these improvements.

iable with time, both throughout a single observing run and from one run to the next, which is consistent with other findings, such as in Krisciunas (1997), who mentions that except for the solar cycle, the most important effect on sky brightness is random short-term variations on timescales of tens of minutes. This makes it difficult to compare sky values from site to site. A more reliable method of comparison would be to amass a large collection of sky surface brightness data over years at each site in order to better understand and remove the short- and long-term variations in sky brightness, which is currently not fully understood. Various site-dependent factors should also be taken into consideration, such as the linear dependence of sky surface brightness on geomagnetic latitude due to Aurora effects in the Van Allen Belt, which mean that low geomagnetic latitudes have somewhat darker skies than higher latitudes. The direction of pointings toward cities can also affect sky brightness, with Tuscon and Phoenix city lights slightly increasing the VATT sky brightness in that direction, by 0.1 mag arcsec$^{-2}$ in $U$ and 0.2 mag arcsec$^{-2}$ in $BVR$. However, measurements made toward the nearest city, Safford, are not measurably brighter than other directions (thanks to dark-sky ordinances in Safford and shielding from the mountain peak at the VATT site). Nightly trends are also seen, with sky brightness values decreasing throughout at least the first half of the night by an amount that depends in part at least on the elevation of the observing site. Mount Graham's high elevation contributes in this and many other ways to darker night skies, and the minimal effect of city lights at this location make Mount Graham a prime dark-sky site that can easily compete with other dark sites around the world.

The FWHM of stars in images we took at the VATT have improved considerably (by 0ʺ.45) since maintenance operations for the summer and fall of 2001 corrected secondary mirror vibrations and improved the telescope pointing map. Figures 7, 8, and 11 and Table 2 show our stellar FWHM results. We were able to get subarcsecond seeing on occasion, especially in short focus (several second) exposures, which are less affected than long object exposures by vibrations, variable atmospheric seeing, and slipping of the telescope out of focus as temperatures change. Because of this, the FWHM values given by focus exposures are closer to the true atmospheric seeing (by about 0ʺ.3) than those from faint object images.

It should also be noted that there may be a significant telescope contribution to the seeing measured at the VATT, and that the atmospheric seeing may be different at other likely locations on Mount Graham, since the presence of trees as tall as the dome around the VATT have a negative impact on the seeing at that telescope. Good seeing is not crucial to our purposes of performing surface photometry on extended galaxies, but observers who desire smaller PSFs should be able to improve on our numbers by focusing more often (at least once an hour, and more often at the beginning of the night, when the temperature is more unstable) and by refocusing for each individual filter rather than using the focus of one filter for all filters. It should also be noted that the seeing is highly dependent on the weather, with strong northeasterly winds contributing to much worse seeing.

V. A. T. was supported in part by the NASA Space Grant Graduate Fellowship at Arizona State University and in part by NASA grants GO-9824.1 and GO-9124.1. R. A. J. acknowledges partial support from NASA grant GO-9892.1. We wish to thank the staff at the VATT, especially Richard Boyle, Matthew Nelson, and Christopher Corbally for their gracious help and support. We also wish to thank our many co-observers: Claudia Chiarenza, Thomas McGrath, Luis Echevarria, Hu Zhan, Seth Cohen, Stephen Odewahn, Richard de Grijs, Corey Bartley, Joe Baker, Jason Mager, and Kazuyuki Tamura. R. A. J. wishes to extend particular thanks to Elizabeth Barton, who was principal investigator on several of the programs for which FWHM measurements are presented in this paper. We also thank the referee, Wes Lockwood, who offered very knowledgeable and helpful comments. On behalf of all MGIO observers, we wish to thank the Tucson and Safford city councils for passing strict low-pressure sodium light ordinances, which make a noticeable difference in the sky brightness at Mount Graham.

## REFERENCES

Benn, C. R., & Ellison, S. L. 1998, NewA Rev., 42, 503
Bertin, E., & Arnouts, S. 1996, AJ, 117, 393
Coulman, C. E. 1985, ARA&A, 23, 19
Fried, D. L. 1965, J. Opt. Soc. Am., 55, 1427
Garstang, R. H. 1989, PASP, 101, 306
Kolmogorov, A. N. 1941, in Selected Works of A. N. Komogorov: Mathematics and its Applications, ed. V. M. Tikhomirov (1991; Dordrecht: Kluwer)
Krisciunas, K. 1997, PASP, 109, 1181
Krisciunas, K., & Schaefer, B. 1991, PASP, 103, 1033
Landolt, A. U. 1992, AJ, 104, 340
Massey, P., & Foltz, C. B. 2000, PASP, 112, 566
Odewahn, S. C., Cohen, S. H., Windhorst, R. A., & Philip, N. S. 2002, ApJ, 568, 539
Patat, F. 2003, A&A, 400, 1183
Roddier, F. 1981, Prog. Opt. 19, 281
Tatarski, V. I. 1961, Wavefront Propagation in a Turbulent Medium (New York: Dover)
Walker, A. 1987, NOAO Newsl., No. 10, 16
Walker, M. 1988, PASP, 100, 496